# Parameter variability of the observed Chandler and annual wobbles based on space-geodetic measurements

Joachim Höpfner

**Summary**

Compared to earlier polar motion (PM) data, the combined Earth orientation series based on precise space-geodetic measurements has a higher accuracy and a higher temporal resolution. Therefore, an analysis of these data should provide considerably more precise results. By using the time series SPACE99 computed by the Jet Propulsion Laboratory (JPL) from 1976 to 2000 with one-day sampling, the Chandler and annual wobbles have been separated by recursive band-pass filtering of the PM coordinates (Höpfner 2002a). In this study, we show the parameter variability of the Chandler and annual wobbles. The results presented include the radii and their direction angles as well as the period lengths and revolution motions over the analysis intervals.

**Zusammenfassung**

*Im Vergleich zu den früheren Polbewegungsdaten haben die Zeitreihen der Erdorientierungsparameter (EOP), die auf der Kombination sehr genauer Messungen mit geodätischen Raumverfahren basieren, eine höhere Genauigkeit und eine höhere zeitliche Auflösung. Deshalb sollte eine Analyse dieser EOP-Daten beträchtlich genauere Resultate liefern. Die Zeitreihe SPACE99, die vom Jet Propulsion Laboratory (JPL) von 1976 bis 2000 mit Tagesabstand berechnet wurde, diente dazu, die Chandler- und Jahreswelle durch rekursive Bandpassfilterung der Polkoordinaten zu separieren (Höpfner 2002a). Wir zeigen die Parametervariabilität beider Wellen. Die Resultate sind die Radien und ihre Richtungswinkel sowie die Periodenlängen und Revolutionsbewegungen für die Analyseintervalle.*

## 1 Introduction

One phenomena resulting from the global dynamics of the Earth are the irregularities in the Earth's rotation. These involve variability in both the rate of rotation and the direction of the rotation axis in space and to the Earth over many timescales. Relative to the terrestrial body-fixed reference frame, variations in the Earth's rotation are measured by changes in the length-of-day (LOD) and polar motion (PM). Research into PM began with the deviation of the equations for the rotation of a rigid body by Euler (1758), followed by further theoretical contributions by Lagrange (1788), Poinsot (1834, 1851) and Peters (1844). Afterwards, intensive efforts at several observatories attempted to determine variations in latitude, however a significant signal could not be resolved. This resulted in a suggestion by Fergola during the 7th General Conference of the European Arc Measurement, i.e., the forerunner of the International Association of Geodesy (IAG), in 1883 to study the problem of PM using latitude observations at observatories located in couples on the same parallel (Jahresbericht Preussen 1884). Finally, in 1888 Küstner determined a real variation of latitude using observations from the Berlin Observatory (Küstner 1888). Moreover, in 1891/92, there was the discovery by Chandler that the periodic latitude variations consisted of two superposed components with periods of ca. 365 and 427 days (Chandler 1891, 1892). Within the scientific community, the problem of PM has raised considerable interest. Activities were intensified and, after an effort covering 10 years, saw the establishment in 1899 of the International Latitude Service (ILS) as the first permanent worldwide scientific cooperation to monitor the motion of the Earth's pole of rotation with respect to six observing sites based on continuous latitude observations (Helmert and Albrecht 1899). In 1962, the ILS was reorganised as the International Polar Motion Service (IPMS). Since the middle of the 1970s, high-precision space geodetic techniques such as VLBI (Very Long Baseline radio Interferometry), LLR (Lunar Laser Ranging), SLR (Satellite Laser Ranging) and from 1992 GPS (Global Positioning System) have been used to measure the Earth orientation parameters. By combining independent measurements, compared to the earlier PM data, the Earth orientation series now available has a higher accuracy and a higher temporal resolution. In 1988, the IPMS was discontinued with the commencement of the International Earth Rotation Service (IERS). To celebrate the centennial of the ILS, the IAU Colloquium 178 »Polar Motion: Historic and Scientific Problems« was held at Cagliari, Italy, in September 1999. The event was hosted by the Stazione astronomica of Cagliari-Carloforte being one of the original ILS observatories. For information on the historical and scientic problems of PM, see the proceedings of this meeting (Dick et al. 2000).

PM time-series data is available from the mid-19th century to the present day. Based on optical astrometry and ILS data, a large number of PM studies have been made in order to derive the main terms of polar motion, including the secular drift of the Earth's pole, Chandler and annual wobbles, for example Wanach (1916, 1919), Kimura (1917), Iijima (1965), Proverbio et al. (1971), Guinot (1972, 1982), Wilson and Vicente (1980), Dickman (1981), Okubo (1982), Chao (1983), Lenhardt and Groten (1987), Nastula et al. (1993), Höpfner (1995a-c, 1996), Vicente and Wilson (1997), Vondrák et al. (1998), Vondrák (1999). Schuh et al. (2001). For more information about

these PM studies and a summary of the main scientific results over past, see Höpfner (2002a) and Höpfner (2000) and references therein.

Independent Earth orientation measurements taken by the space-geodetic techniques have been combined by the Jet Propulsion Laboratory (JPL) at daily intervals (see e.g. Gross 2000). This time series, labelled SPACE99, have been used as input data of our previous PM studies that dealt with periodic motions ranging between about 650 and 45 days (Höpfner 2002a, 2002b, Höpfner 2002). The data used was from Sept. 28.0, 1976 to Jan. 22.0, 2000, i.e. Modified Julian Date (MJD) from 43049.0 to 51565.0 (Gross 2000). We will now briefly review these papers:

First, the major periodic PM components, in particular the Chandler and annual wobbles, were separated by recursive band-pass filtering of the PM coordinates. Then, based on least-squares fit, the parameters and their uncertainties for the different equivalent representation forms (trigonometric, exponential and geometric) and portion types (oscillation of the real and imaginary parts, circular and elliptical) were computed at epochs with quarterly (annual) sampling. This resulted in the characteristics and time evolution of the Chandler and annual wobbles (Höpfner 2002a).

Continuing this work, after removing the low-frequency component and the Chandler and annual wobbles from the PM coordinates, the resulting residual time series was used to separate out the substantially smaller polar motions by band-pass filtering, in particular the quasi-biennial, 300-day, semi-Chandler, semi-annual, 4-month, 90-day, 2-month and 1.5-month wobbles. It was found that the persistence of the oscillations becomes less with increasing frequency (Höpfner 2002b).

In order to quantify and better describe the parameter variability of these PM components over time, particularly the eight oscillations with periods ranging between ca. 650 and 45 days, we computed the radii, direction angles and period lengths from the periodic terms filtered out from the time series. The results clearly showed the characteristics and time evolution of the periodic PM components (Höpfner 2002).

Motivated by the high quality of the results obtained for the eight observed PM components with smaller amplitudes (Höpfner 2002), the time series filtered out for the Chandler and annual wobbles (Höpfner 2002a) have been processed in this work by the same method.

## 2 Data processing and results

As already mentioned, we refer to our previous results for the Chandler and annual terms filtered out from the combined Earth orientation series SPACE99 (JPL). Both periodic motions were separated by recursive band-pass filtering for the $x_1$- and $x_2$-components with one-day sampling (Höpfner 2002a).

In complex notation, the periodic components $x_f(t)$ with a frequency $f$ and the time variable $t$ of the PM have the form

$$x_f(t) = x_{1,f}(t) \; + \; i \;\; x_{2,f}(t) \; . \tag{1}$$

Concerning the axes of the coordinates, note that the $x_1$-axis points towards the Greenwich meridian, and the $x_2$-axis towards 90° East longitude. That is, we use the mathematical coordinate system with $x_1 = x$ and $x_2 = -y$ where $x, y$ are the Celestial Ephemeris Pole (CEP) relative to the IERS Reference Pole (IRP) (see e.g. IERS (2000)). A perspective representation of the filtered 2-D Chandler and annual wobbles by elliptic spiral curves with time can be found in Höpfner (2002a). For the time intervals of the oscillations, see Table 1.

Based on considerations of periodic polar motions in the polar coordinate system, the data processing for the Chandler and annual wobbles includes the following two steps:

(1) Computing the radii $r_f(t)$ according to

$$\begin{aligned} r_f(t) = |x_f(t)| &= |x_{1,f}(t) \; + \; i \;\; x_{2,f}(t)| \\ &= \left( x_{1,f}(t)^2 + x_{2,f}(t)^2 \right)^{\frac{1}{2}} \end{aligned} \tag{2}$$

and their direction angles $\gamma_f(t)$ according to

$$\gamma_f(t) = \arctan \frac{x_{2,f}(t)}{x_{1,f}(t)} \; . \tag{3}$$

(2) Determining the semi-major axes $a$ and semi-minor axes $b$ as the maxima and minima of the radii $r_f(t)$ according to

$$\begin{aligned} a = r_f(t_a) = \max\{r_f(t)\} \quad \text{and} \\ b = r_f(t_b) = \min\{r_f(t)\} \; , \end{aligned} \tag{4}$$

their directions $\gamma_a$ and $\gamma_b$ according to

$$\gamma_a = \gamma_f(t_a) \quad \text{and} \quad \gamma_b = \gamma_f(t_b) \; , \tag{5}$$

and the period lengths $T$ of an elliptic motion as the time differences at the direction angles $\gamma_f(t)$, being 0° and 360°.

| Wobble | Time interval (MJD) | Time interval (calendar days) |
|---|---|---|
| Chandler | 44004.0 ... 50610.0 | 1979/05/11 ... 1997/06/11 |
| Annual | 43843.0 ... 50771.0 | 1978/12/01 ... 1997/11/19 |

Table 1: Time intervals of the Chandler and annual wobbles filtered out from the combined Earth orientation series SPACE99 (JPL) given in MJD and calendar days

| Wobble | Period (days) | Motion direction | Type | Numerical eccentricity | Semi-major axis (mas) | Direction of the semi-major axis | Semi-minor axis (mas) |
|---|---|---|---|---|---|---|---|
| Chandler | 423.0 ... 438.0 | prograde | quasi-circular | 0.00 ... 0.24 | 152.7 ... 202.4 | 50.3° ... 199.9° | 150.3 ... 200.2 |
| Annual | 355.0 ... 371.0 | prograde | elliptic | 0.23 ... 0.50 | 62.1 ... 95.6 | 154.2° ... 193.6° | 55.1 ... 87.1 |

Table 2: Characteristics of the Chandler and annual wobbles relative to the JPL system

The smaller the difference between the semi-major and semi-minor axes, the more circular is the periodic motion; while the larger the difference, the more elliptic is the motion. Also, the numerical eccentricity $\epsilon$ used as a dimensionless measure for the ellipticity of a periodic motion is computed according to

$$\epsilon = \frac{(a^2 - b^2)^{\frac{1}{2}}}{a}. \qquad (6)$$

If $\epsilon = 0$, then there is a circular motion; if $0 < \epsilon < 1$, then there is an elliptic motion. The closer $\epsilon$ is to 0, the more circular is its motion, while the closer $\epsilon$ is to 1, the more elliptic is its motion.

Note that the semi-major and semi-minor axes and their directions are determined for actual time points of a periodic component in the polar coordinate system.

Figure 1 presents the variability in the parameters of the Chandler wobble, while Fig. 2 shows the same for the annual wobble. In these figures, the radial variation is at the top, with the superior envelope indicating the change in the semi-major axis and the inferior envelope the change in the semi-minor axis. The directions of the radii are in the centre, with markers indicating the direction angles of the semi-major and semi-minor axes. The period variability is shown at the bottom, with the dashed line indicating a baseline of 435 days for the Chandler wobble in Fig. 1 and of 365 days for the annual wobble in Fig. 2. Figure 3 shows the time evolutions of the Chandler wobble over the analysis interval in terms of the revolution motions in 16 pictures, and, in Fig. 4, the same for the annual wobble in 20 pictures. A full cycle is shown in each picture, except in the first and last pictures. Note that the date given in MJD is the start of the curve and the arrow indicates the direction of motion. For the date of the end of the curve, see the following picture.

A summary of the relevant characteristics of the Chandler and annual wobbles is given in Table 2, in particular the ranges in period length, the direction and the type of motion, numerical eccentricity, semi-major axis, direction of the semi-major axis and semi-minor axis. In order to better assess the results, we have compiled the features of the Chandler and annual wobbles relative to each cycle in Tables 3 and 4, with time interval, period length, extremes of the radii (amplitudes), numerical eccentricity, radius change over each time interval and a more specified motion type. Table 5 presents the uncertainties associated with each of the Chandler and annual wobble parameters and in particular of the semi-major and semi-minor axes and their directions which were estimated by means of the neighbouring values.

## 3 Discussion of the results

In general, when considering a periodic motion in the polar coordinate system, the following characteristics should be noted:

- If the direction angle increases, then the motion is prograde, i.e. counter-clockwise. If it decreases, then the motion is retrograde, i.e. clockwise.
- Each direction course of 0° to 360° (or vice versa of 360° to 0°) describes an elapsed prograde (or retrograde) revolution of the PM component of interest, with its turning-points indicating the extreme sites (maxima and minima of the radii) of the component.
- The more straight the direction course over a revolution, the more circular is the periodic motion. Conversely, the more curved the direction course, the more elliptic is the motion.

Compared to previous PM studies that are based on optical astrometric measurements (see the Introduction), those based on space-geodetic measurements are of a higher quality. However, concerning our solutions for the Chandler and annual wobbles, it should be noted that a few of the estimates at the beginning and end of the resulting time series may be less accurate because of edge effects in the recursive band-pass filtering.

The following discussion of the results will be separately on the Chandler and annual wobbles. It includes a comparison with our previous estimates based on a moving least-squares fit (Höpfner 2002a).

### Chandler wobble (Figs. 1 and 3, and Table 3)

The Chandler wobble is resolved over nearly 16 cycles between 1979–1997. At the beginning (MJD 44004.0, May 11, 1979), it has a radius of 153.35 mas and decreases by about 2 mas over 252 days until MJD 44256.0, i.e. Jan. 1980 (in the 1st picture of Fig. 3). The motion course then increases and again decreases in radius over different intervals. In particular, there exists an increase from MJD 44257.0 to 45977.0, i.e. from Jan. 1980 to Oct. 1984 (pictures (2) to (5)) and a decrease from MJD 45978.0 to 46845.0, i.e. from Oct. 1984 to Feb. 1987 (pictures (6)

and (7)). After that, the radius again increases, namely from MJD 46846.0 to 49455.0, i.e. from Feb. 1987 to April 1994 (plotted in pictures (8) to (13)). Then, during the interval from MJD 49456.0 to 50610.0, i.e. April 1994 to June 1997, the radius again decreases (plotted in pictures (14) to (16)). The magnitude of the radial changes as obtained over each cycle are presented in Table 3.

As for the direction and type of motion, we see that the Chandler motion is prograde (i.e. counter-clockwise) and variable between circular and a little oval over these cycles. The reason for a quasi-circular motion is that the semi-major axis (that varies between 152.7 to 202.4 mas) and the semi-minor axis (that varies between 150.3 to 200.2 mas) only somewhat differ. Especially, noticeable is the difference range between 0.0 (in the 3rd and 15th cycles) and 5.4 mas (in the 9th cycle) resulting in a numerical eccentricity $\epsilon$ between 0 and 0.24. Concerning the orientation of the Chandler motion relative to the semi-major axis, there is considerable variability, namely between 50.3°and 199.9°, obtained for the low-elliptic cycles. An elliptic motion cycle should exhibit two maximum and two minimum radius values. However, if a cycle elapsed as a quasi-circular spiral, any number of them could be missing. Some examples for this are the cycles plotted in the pictures (2) to (4), (11) and (14), (15). In two cases (pictures (3) and (15)), there are no maximum and minimum radii values and therefore each cycle is elapsed in terms of a pure circular spiral; the cycle of (3) has a radius increasing by 14.33 mas and that of (15) a radius decreasing by 17.37 mas.

Concerning the variation in the Chandler period ranging between 423 and 438 days with an estimated uncertainty of ±0.5 days (bottom of Fig. 1), there is a similarity to our previous result obtained by using a method based on the maximum, zero crossing and minimum of a periodic function, to the filtered periodic terms separately for the $x_1$- and $x_2$-components. Compared to the change in radius (see top of Fig. 1) of the Chandler wobble, the change in period (see bottom of Fig. 1) is similar in its time dependence, i.e. a correlation between both parameters exists as found in previous PM studies such as Iijima (1965), Proverbio et al. (1971) and Vondrák (1999).

### Annual wobble (Figs. 2 and 4, and Table 4)

For the period 1978-1997, the annual wobble has been separated into about 19 cycles. Concerning the change in radius, there are following motion courses: Beginning with a radius of 67.97 mas at MJD 43843.0 (Dec. 1, 1978), an increase in radius occurs over six cycles until MJD 45939.0, i.e. from Dec. 1978 to Aug. 1984 (plotted in the pictures (1) to (6)). After that, there is a decrease between MJD 45940.0 to 49241.0, i.e. from Aug. 1984 to Sept. 1993 (plotted in the pictures (7) to (15)). Then, in pictures (16) and (17), we see that the radius again increases (between MJD 49242.0 to 49964.0, i.e. from Sept. 1993 to Sept. 1995), and, in pictures (18) to (20), that it again decreases (between MJD 49965.0 to 50771.0, i.e. from Sept. 1995 to Nov. 1997). See Table 4 for the values in the radial range over each cycle.

Compared to the Chandler wobble, the annual motion is also prograde, but the motion type becomes more elliptic over the cycles. During the analysis interval, its semi-major axis varies between 62.1 and 95.6 mas and its semi-minor axis between 55.1 to 87.1 mas. The difference between the semi-major and semi-minor axes ranges from 2.03 (in the 2nd cycle) to 9.19 mas (in the 8th cycle), and consequently the numerical eccentricity $\epsilon$ from 0.23 to 0.50. For the orientation of the elliptic motion, the direction of the semi-major axis only varies by 39.4°, between 154.2°and 193.6°, over the analysis interval with a systematic shift of a few degrees from cycle to cycle, alternatively positive and negative over several cycles.

The annual period varies from 355 to 371 days with an estimated uncertainty of ±0.5 days (bottom of Fig. 2). This result coincides with previously found results (derived in the same manner as for the Chander period). A comparison of the semi-axis curves with the period curve shows that there are similar changes, i.e. the shorter (longer) periods of the annual motion are probably associated with smaller (larger) radii (amplitudes). This correlation is similar to that found for the Chandler wobble.

Finally, it is necessary to compare and to judge the results of this paper with those obtained by using a least-squares fit with quarterly sampling (Höpfner 2002a). Some special characteristics for the results of the parameters of an elliptic motion derived by the two methods exist and are compiled in Table 6. Comparing the variations in the semi-major and semi-minor axes and directions of the semi-major axes for the Chandler and annual wobbles obtained from both methods, we can say that there is an excellent agreement between them. Moreover, as can be seen from Table 5, the uncertainties in the elliptic parameters estimated from neighbouring values are very small. Therefore, the method used here is well suited for studying the parameter variability of the observed Chandler and annual wobbles based on space-geodetic measurements.

For a comparison of our results with other recent studies, e.g. Nastula et al. (1993), Höpfner (1995a-c, 1996), Vondrák (1999) and Schuh et al. (2001), see Höpfner (2002a). We found that there are either no or only relatively short common intervals and in the cases where there was a common time interval, the estimates are similar.

## 4 Concluding remarks

Analogous to Höpfner (2002), this study of the Chandler and annual wobbles is based on the considerations of the periodic PM components in the polar coordinate system. The results obtained from the filtered Chandler and annual terms relative to the JPL system are radii, direction

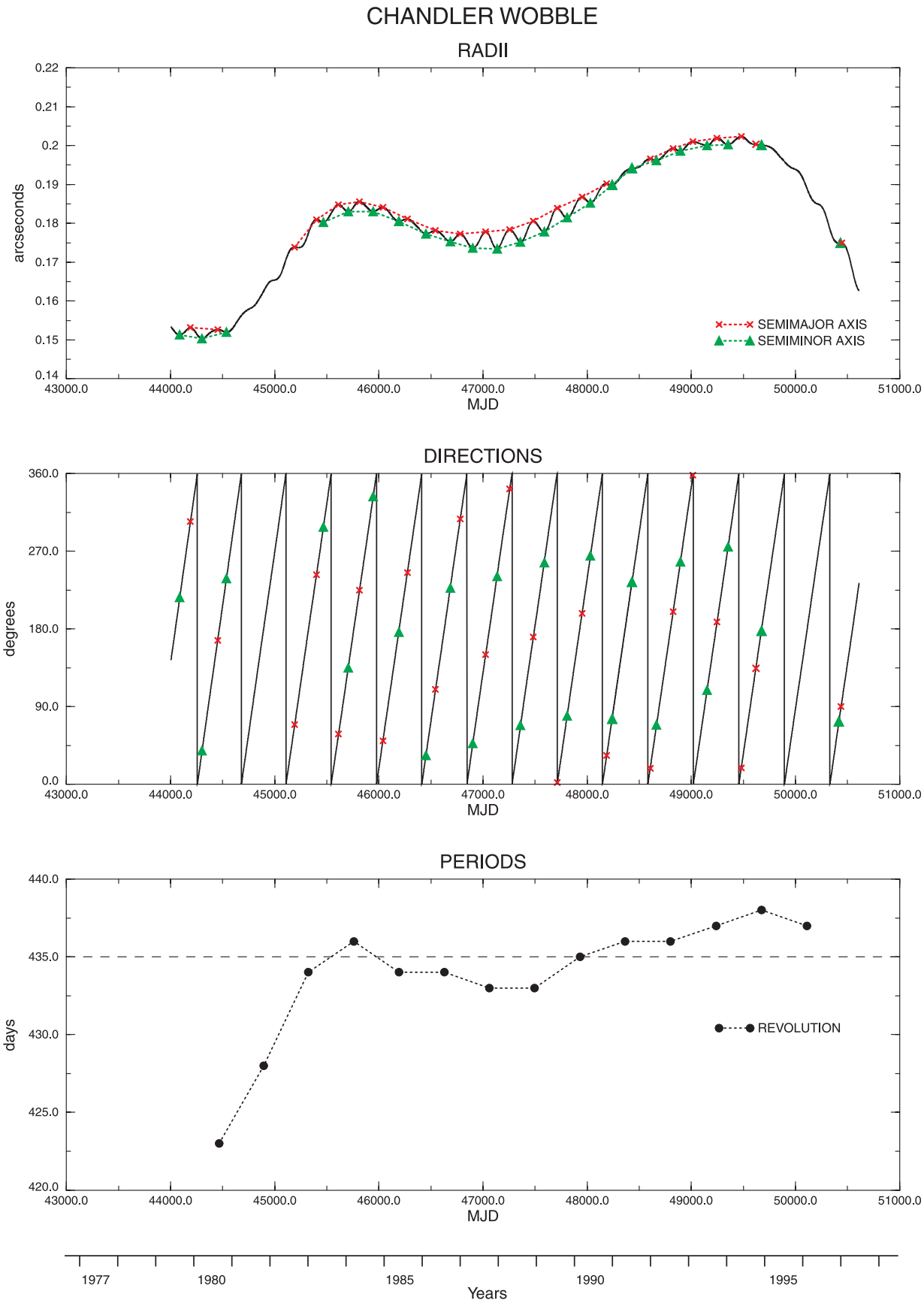


Fig. 1: Variations in the parameters of the Chandler wobble.
The curves shown are: Radii, semi-major and semi-minor axes (top), directions of the radii (centre) and periods (bottom). The markers used are x in red at the maxima and triangles in green at the minima. In the period plot, each filled circle indicates the period length of an elapsed revolution.

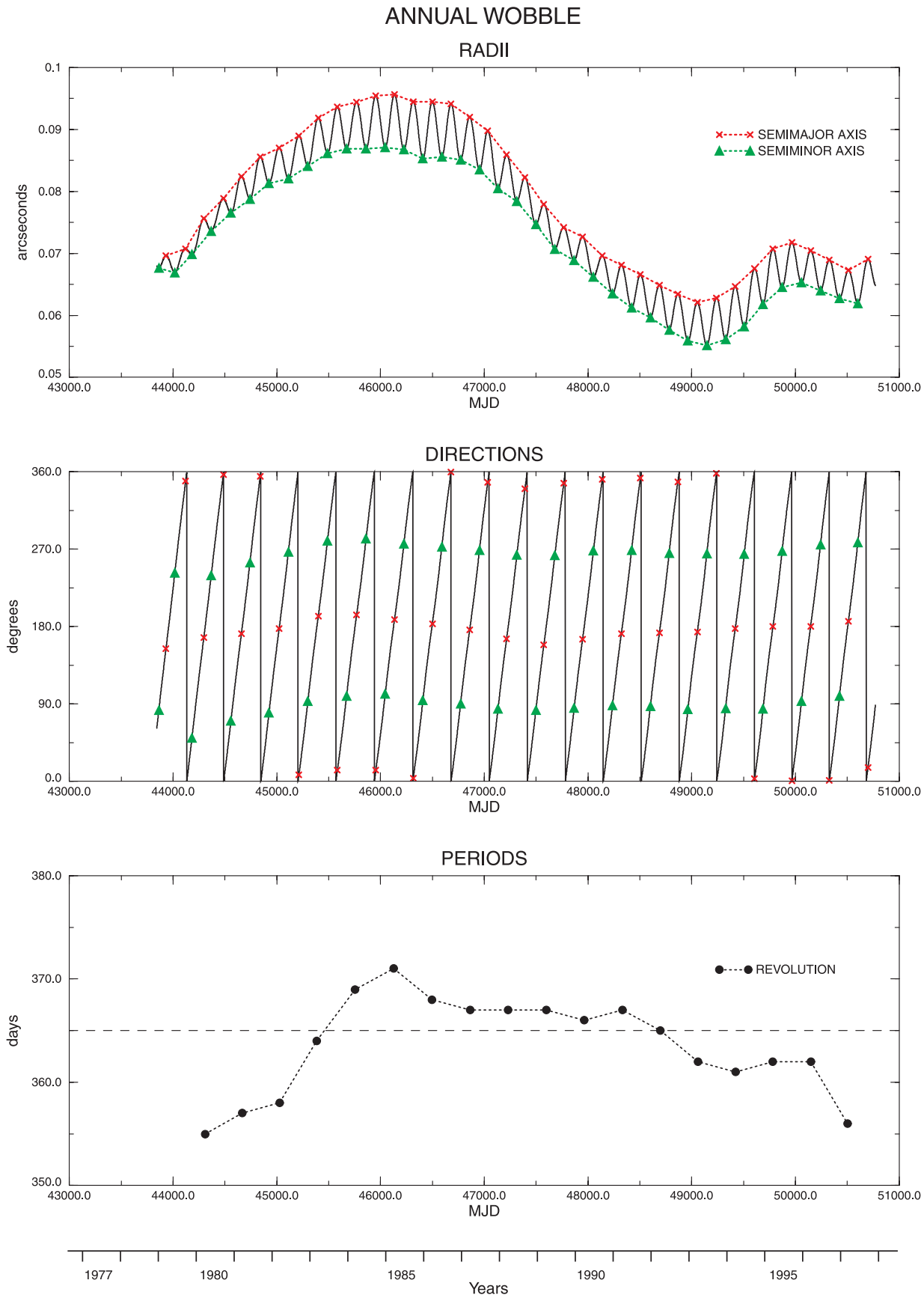


Fig. 2: Variations in the parameters of the annual wobble.
The curves shown are: Radii, semi-major and semi-minor axes (top), directions of the radii (centre) and periods (bottom). The markers used are x in red at the maxima and triangles in green at the minima. In the period plot, each filled circle indicates the period length of an elapsed revolution.

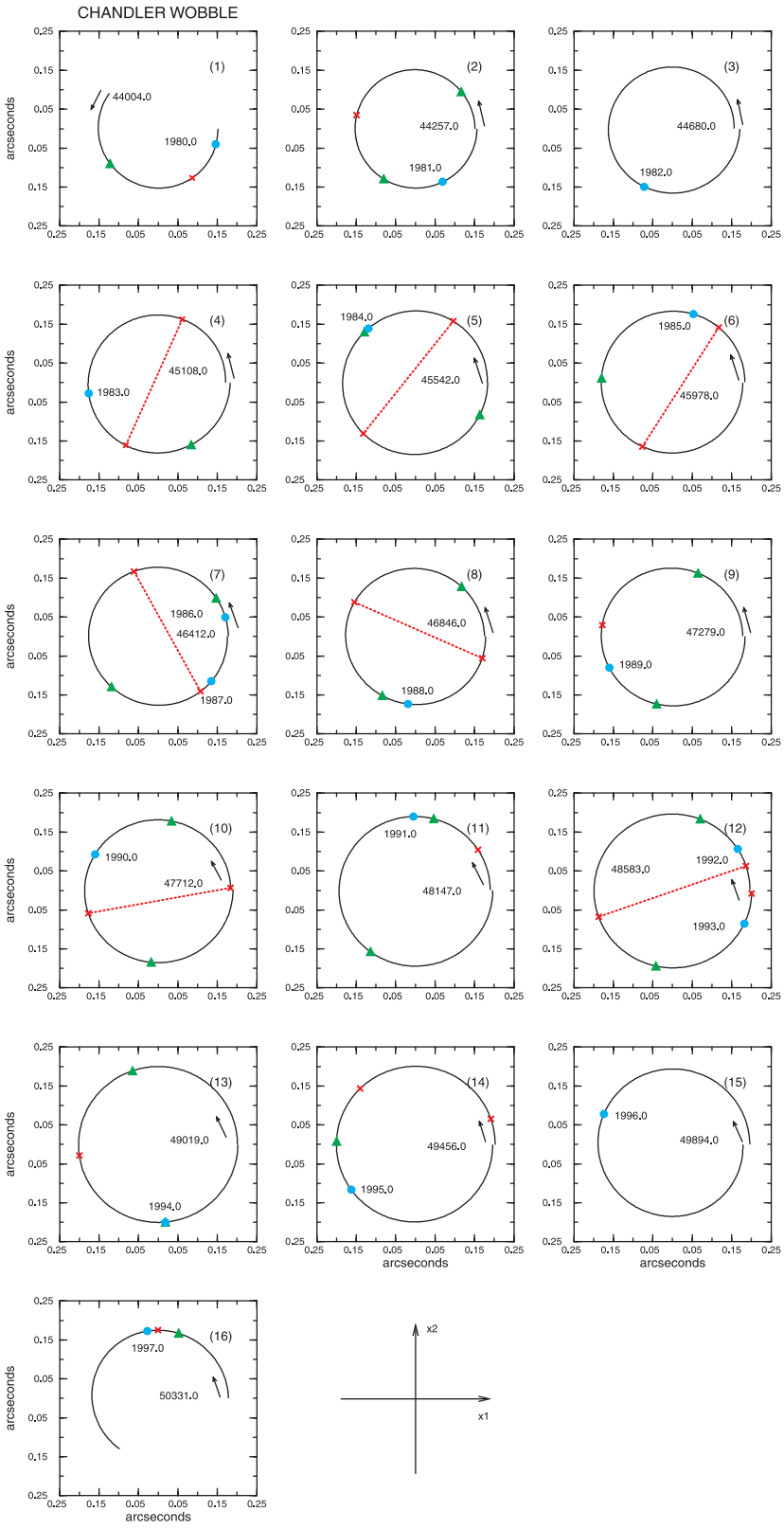


Fig. 3: The Chandler wobble.
The curves shown are the revolution motions over the analysis interval (from left to right and from top to bottom). The $x_1$-axis points towards the Greenwich meridian, and the $x_2$-axis towards 90°E longitude. The markers used are x in red at the maxima and triangles in green at the minima. Also indicated is the beginning of a year by a filled circle in cyan. For the revolution times in years, see Fig. 1.

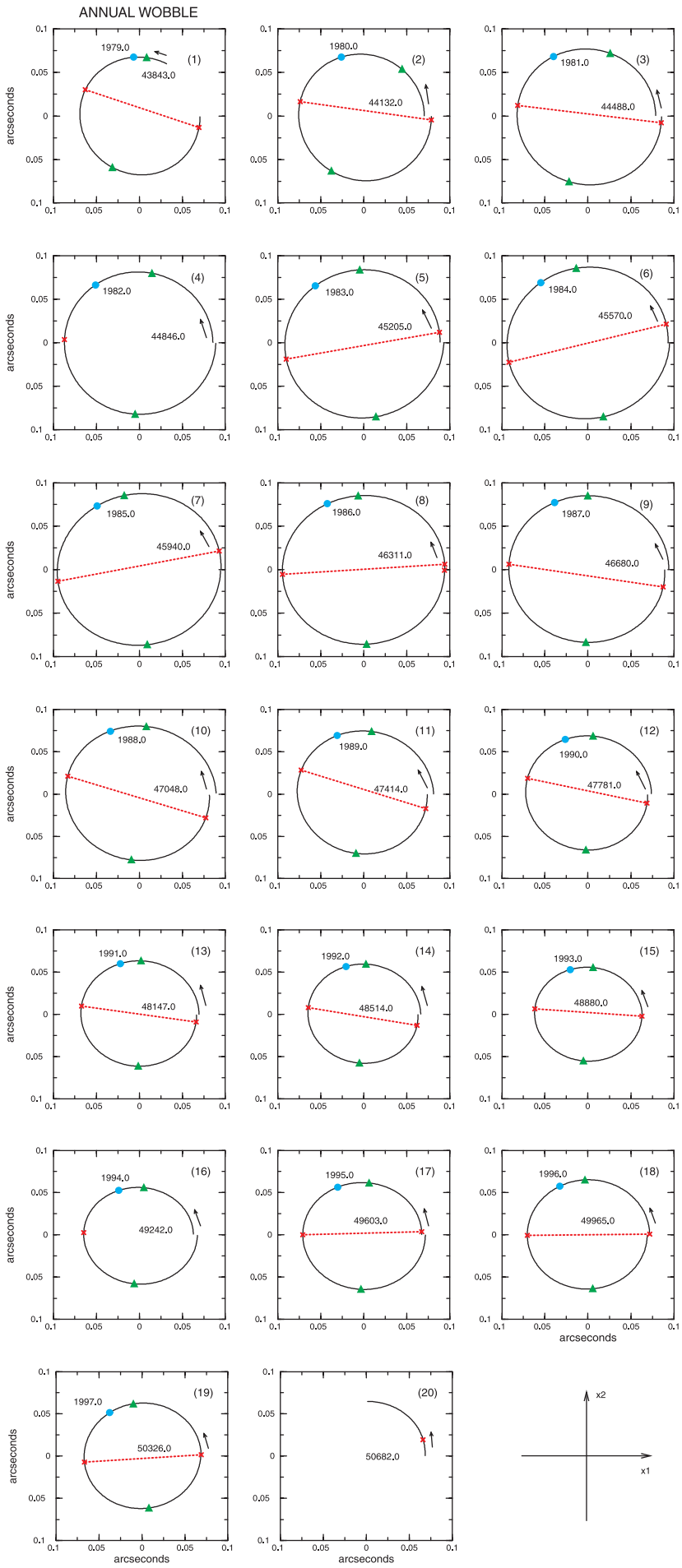


Fig. 4: The annual wobble.
The curves shown are the revolution motions over the analysis interval (from left to right and from top to bottom). The $x_1$-axis points towards the Greenwich meridian, and the $x_2$-axis towards 90°E longitude.
The markers used are x in red at the maxima and triangles in green at the minima. Also indicated is the beginning of a year by a filled circle in cyan. For the revolution times in years, see Fig. 2.

| Cycle | Time interval (MJD) | Period (days) | Extreme a/b | Time point (MJD) | Radius (mas) | Direction | Numerical eccentricity | Radius change over the time interval (mas) | Motion type |
|---|---|---|---|---|---|---|---|---|---|
| 01 | 44004.0 ... 44256.0 | (252.0) | b | 44088.0 | 151.30 | 216.45° | | -2.02 | oval |
| | | | a | 44191.0 | 153.17 | 304.42° | 0.156 | | |
| 02 | 44257.0 ... 44679.0 | 423.0 | b | 44302.0 | 150.31 | 38.99° | | +4.97 | oval |
| | | | a | 44452.0 | 152.70 | 166.91° | 0.176 | | |
| | | | b | 44536.0 | 151.97 | 238.27° | 0.098 | | |
| 03 | 44680.0 ... 45107.0 | 428.0 | | 44680.0 | 156.29 | 0.33° | | +14.33 | circular-spiral |
| | | | | 45107.0 | 170.62 | 359.61° | | | |
| 04 | 45108.0 ... 45541.0 | 434.0 | a | 45192.0 | 173.85 | 69.49° | | +11.84 | oval |
| | | | a | 45401.0 | 180.96 | 242.92° | | | |
| | | | b | 45467.0 | 180.25 | 297.67° | 0.088 | | |
| 05 | 45542.0 ... 45977.0 | 436.0 | a | 45613.0 | 184.83 | 58.51° | | +0.75 | quasi-circular |
| | | | b | 45705.0 | 183.02 | 134.72° | 0.140 | | |
| | | | a | 45814.0 | 185.60 | 224.86° | 0.166 | | |
| | | | b | 45945.0 | 183.05 | 333.07° | 0.165 | | |
| 06 | 45978.0 ... 46411.0 | 434.0 | a | 46038.0 | 184.09 | 50.31° | | -5.50 | oval |
| | | | b | 46190.0 | 180.52 | 176.31° | 0.196 | | |
| | | | a | 46273.0 | 181.14 | 245.10° | 0.083 | | |
| 07 | 46412.0 ... 46845.0 | 434.0 | b | 46452.0 | 177.29 | 33.78° | | -2.01 | quasi-circular |
| | | | a | 46544.0 | 178.13 | 109.99° | 0.097 | | |
| | | | b | 46685.0 | 175.28 | 227.44° | 0.178 | | |
| | | | a | 46781.0 | 177.28 | 307.27° | 0.150 | | |
| 08 | 46846.0 ... 47278.0 | 433.0 | b | 46902.0 | 173.67 | 47.69° | | +2.72 | elliptic |
| | | | a | 47025.0 | 177.87 | 150.23° | 0.216 | | |
| | | | b | 47134.0 | 173.44 | 240.95° | 0.222 | | |
| | | | a | 47256.0 | 178.33 | 341.91° | 0.233 | | |
| 09 | 47279.0 ... 47711.0 | 433.0 | b | 47360.0 | 175.16 | 68.39° | | +5.87 | elliptic |
| | | | a | 47483.0 | 180.54 | 170.60° | 0.242 | | |
| | | | b | 47587.0 | 177.78 | 256.76° | 0.174 | | |
| 10 | 47712.0 ... 48146.0 | 435.0 | a | 47714.0 | 183.91 | 2.20° | | +5.75 | oval |
| | | | b | 47807.0 | 181.41 | 79.12° | 0.164 | | |
| | | | a | 47951.0 | 186.73 | 198.24° | 0.237 | | |
| | | | b | 48031.0 | 185.24 | 264.45° | 0.126 | | |
| 11 | 48147.0 ... 48582.0 | 436.0 | a | 48187.0 | 190.22 | 33.41° | | +6.78 | quasi-circular |
| | | | b | 48238.0 | 189.82 | 75.64° | 0.065 | | |
| | | | b | 48430.0 | 194.11 | 234.24° | | | |
| 12 | 48583.0 ... 49018.0 | 436.0 | a | 48605.0 | 196.59 | 18.71° | | +4.57 | quasi-circular |
| | | | b | 48666.0 | 196.20 | 68.99° | 0.063 | | |
| | | | a | 48825.0 | 199.27 | 199.88° | 0.175 | | |
| | | | b | 48895.0 | 198.57 | 257.78° | 0.084 | | |
| | | | a | 49016.0 | 201.05 | 357.79° | 0.157 | | |
| 13 | 49019.0 ... 49455.0 | 437.0 | b | 49151.0 | 199.99 | 109.03° | | +1.10 | oval |
| | | | a | 49247.0 | 201.93 | 188.00° | 0.138 | | |
| | | | b | 49353.0 | 200.21 | 275.25° | 0.130 | | |
| 14 | 49456.0 ... 49893.0 | 438.0 | a | 49479.0 | 202.36 | 19.02° | | -6.24 | circular-spiral |
| | | | a | 49619.0 | 200.30 | 134.27° | | | |
| | | | b | 49672.0 | 200.15 | 177.88° | 0.039 | | |
| 15 | 49894.0 ... 50330.0 | 437.0 | | 49894.0 | 195.90 | 0.34° | | -17.37 | circular-spiral |
| | | | | 50330.0 | 178.53 | 359.66° | | | |
| 16 | 50331.0 ... 50610.0 | (279.0) | b | 50417.0 | 174.90 | 72.72° | | -15.78 | circular-spiral |
| | | | a | 50438.0 | 174.92 | 90.13° | 0.015 | | |

Table 3: Features of the Chandler wobble cycles relative to the JPL system.
Note: a, maximum of the radii (semi-major axis); b, minimum of the radii (semi-minor axis).
A positive (negative) radius change indicates that the motion course increases (decreases).

| Cycle | Time interval (MJD) | Period (days) | Extreme a/b | Time point (MJD) | Radius (mas) | Direction | Numerical eccentricity | Radius change over the time interval (mas) | Motion type |
|---|---|---|---|---|---|---|---|---|---|
| 01 | 43843.0 ... 44131.0 | (288.0) | b | 43862.0 | 67.60 | 82.73° | | +2.66 | elliptic |
| | | | a | 43931.0 | 69.65 | 154.20° | 0.241 | | |
| | | | b | 44016.0 | 66.89 | 242.09° | 0.279 | | |
| | | | a | 44121.0 | 70.72 | 349.27° | 0.325 | | |
| 02 | 44132.0 ... 44487.0 | 355.0 | b | 44181.0 | 69.85 | 50.24° | | +8.22 | |
| | | | a | 44296.0 | 75.63 | 167.32° | 0.383 | | |
| | | | b | 44367.0 | 73.60 | 239.30° | 0.230 | | |
| | | | a | 44484.0 | 78.86 | 356.65° | 0.359 | | |
| 03 | 44488.0 ... 44845.0 | 357.0 | b | 44557.0 | 76.52 | 70.14° | | +6.73 | |
| | | | a | 44658.0 | 82.43 | 171.50° | 0.372 | | |
| | | | b | 44740.0 | 78.77 | 253.92° | 0.295 | | |
| | | | a | 44840.0 | 85.61 | 354.75° | 0.392 | | |
| 04 | 44846.0 ... 45204.0 | 358.0 | b | 44924.0 | 81.32 | 79.51° | | +3.33 | |
| | | | a | 45022.0 | 87.05 | 177.60° | 0.357 | | |
| | | | b | 45111.0 | 82.06 | 266.53° | 0.334 | | |
| 05 | 45205.0 ... 45569.0 | 364.0 | a | 45213.0 | 88.99 | 7.92° | | +4.31 | more elliptic |
| | | | b | 45299.0 | 84.06 | 93.10° | 0.328 | | |
| | | | a | 45399.0 | 91.87 | 191.83° | 0.403 | | |
| | | | b | 45488.0 | 86.15 | 279.49° | 0.347 | | |
| 06 | 45570.0 ... 45939.0 | 369.0 | a | 45584.0 | 93.62 | 13.26° | | +1.67 | |
| | | | b | 45672.0 | 86.87 | 99.00° | 0.373 | | |
| | | | a | 45769.0 | 94.40 | 193.55° | 0.391 | | |
| | | | b | 45860.0 | 86.88 | 281.89° | 0.391 | | |
| 07 | 45940.0 ... 46310.0 | 371.0 | a | 45954.0 | 95.43 | 12.99° | | -0.56 | |
| | | | b | 46045.0 | 87.11 | 101.74° | 0.408 | | |
| | | | a | 46134.0 | 95.62 | 187.94° | 0.412 | | |
| | | | b | 46225.0 | 86.73 | 276.13° | 0.421 | | |
| 08 | 46311.0 ... 46679.0 | 368.0 | a | 46315.0 | 94.50 | 3.80° | | -0.33 | |
| | | | b | 46408.0 | 85.31 | 94.37° | 0.430 | | |
| | | | a | 46499.0 | 94.47 | 183.27° | 0.430 | | |
| | | | b | 46590.0 | 85.58 | 272.31° | 0.424 | | |
| | | | a | 46679.0 | 94.13 | 359.65° | 0.416 | | |
| 09 | 46680.0 ... 47047.0 | 367.0 | b | 46771.0 | 85.11 | 90.04° | | -4.77 | more elliptic |
| | | | a | 46859.0 | 92.02 | 176.10° | 0.380 | | |
| | | | b | 46953.0 | 83.47 | 268.36° | 0.421 | | |
| | | | a | 47033.0 | 89.78 | 347.36° | 0.368 | | |
| 10 | 47048.0 ... 47413.0 | 367.0 | b | 47132.0 | 80.45 | 84.19° | | -7.77 | |
| | | | a | 47215.0 | 85.92 | 165.69° | 0.351 | | |
| | | | b | 47314.0 | 78.41 | 263.22° | 0.409 | | |
| | | | a | 47392.0 | 82.27 | 340.01° | 0.303 | | |
| 11 | 47414.0 ... 47780.0 | 367.0 | b | 47497.0 | 74.68 | 82.84° | | -7.51 | most elliptic |
| | | | a | 47574.0 | 77.92 | 158.69° | 0.285 | | |
| | | | b | 47680.0 | 70.70 | 262.68° | 0.420 | | |
| | | | a | 47766.0 | 74.21 | 346.59° | 0.304 | | |
| 12 | 47781.0 ... 48146.0 | 366.0 | b | 47866.0 | 68.90 | 85.09° | | -4.40 | |
| | | | a | 47947.0 | 72.68 | 165.05° | 0.318 | | |
| | | | b | 48052.0 | 66.18 | 268.09° | 0.413 | | |
| | | | a | 48137.0 | 69.63 | 351.12° | 0.311 | | |
| 13 | 48147.0 ... 48513.0 | 367.0 | b | 48236.0 | 63.53 | 88.28° | | -3.03 | |
| | | | a | 48321.0 | 68.09 | 171.63° | 0.360 | | |
| | | | b | 48420.0 | 61.20 | 268.74° | 0.438 | | |
| | | | a | 48505.0 | 66.57 | 352.47° | 0.393 | | |
| 14 | 48514.0 ... 48879.0 | 365.0 | b | 48601.0 | 59.63 | 87.29° | | -3.29 | |
| | | | a | 48688.0 | 64.87 | 172.68° | 0.394 | | |
| | | | b | 48782.0 | 57.65 | 265.20° | 0.458 | | |
| | | | a | 48866.0 | 63.43 | 348.30° | 0.417 | | |

| Cycle | Time interval (MJD) | Period (days) | Extreme a/b | Time point (MJD) | Radius (mas) | Direction | Numerical eccentricity | Radius change over the time interval (mas) | Motion type |
|---|---|---|---|---|---|---|---|---|---|
| 15 | 48880.0 ... 49241.0 | 362.0 | b | 48963.0 | 55.88 | 83.91° | | -0.26 | most elliptic |
| | | | a | 49054.0 | 62.09 | 173.86° | 0.436 | | |
| | | | b | 49145.0 | 55.12 | 264.57° | 0.460 | | |
| | | | a | 49239.0 | 62.83 | 358.13° | 0.480 | | |
| 16 | 49242.0 ... 49602.0 | 361.0 | b | 49326.0 | 56.12 | 84.72° | | +4.70 | most elliptic |
| | | | a | 49419.0 | 64.67 | 177.54° | 0.497 | | |
| | | | b | 49506.0 | 58.15 | 264.08° | 0.438 | | |
| 17 | 49603.0 ... 49964.0 | 362.0 | a | 49606.0 | 67.55 | 3.08° | | +4.24 | |
| | | | b | 49687.0 | 61.79 | 83.98° | 0.404 | | |
| | | | a | 49783.0 | 70.73 | 179.97° | 0.487 | | |
| | | | b | 49871.0 | 64.52 | 267.42° | 0.410 | | |
| 18 | 49965.0 ... 50325.0 | 362.0 | a | 49965.0 | 71.77 | 0.80° | | -2.84 | |
| | | | b | 50058.0 | 65.27 | 92.97° | 0.416 | | |
| | | | a | 50146.0 | 70.48 | 180.32° | 0.377 | | |
| | | | b | 50241.0 | 64.00 | 274.94° | 0.419 | | |
| 19 | 50326.0 ... 50681.0 | 356.0 | a | 50327.0 | 68.94 | 1.31° | | -0.45 | |
| | | | b | 50424.0 | 62.71 | 99.03° | 0.415 | | |
| | | | a | 50510.0 | 67.27 | 185.95° | 0.362 | | |
| | | | b | 50601.0 | 61.93 | 277.49° | 0.390 | | |
| 20 | 50682.0 ... 50771.0 | (89.0) | a | 50699.0 | 69.08 | 16.30° | | -3.72 | |

Table 4: Features of the annual wobble cycles relative to the JPL system.
Note: a, maximum of the radii (semi-major axis); b, minimum of the radii (semi-minor axis).
A positive (negative) radius change indicates that the motion course increases (decreases).

| Wobble | Semi-major axis (mas) | Direction of the semi-major axis | Semi-minor axis (mas) | Direction of the semi-minor axis |
|---|---|---|---|---|
| Chandler | $< \pm 0.005$ | $\pm 0.6^{o}$ | $< \pm 0.005$ | $\pm 0.6^{o}$ |
| Annual | $< \pm 0.005$ | $\pm 0.6^{o}$ | $< \pm 0.005$ | $\pm 0.8^{o}$ |

Table 5: Uncertainties in the elliptic parameters for the Chandler and annual wobbles

| Characteristic | Results of this paper | Results from a moving least-squares fit |
|---|---|---|
| Time reference | Time points | Mean epochs |
| Uncertainty | From neighbouring values | Standard deviation |

Table 6: Special characteristics for the results of the parameters of an elliptic motion derived by two methods

angles and period lengths. For the radial variation over time, the superior envelope indicates the change in the semi-major axis and the inferior envelope the change in the semi-minor axis. Compared with the results from a moving least-squares fit, the extremes (semi-major and semi-minor axes) and their directions of the elliptic motions are referred to actual time points. The results show the characteristics and time evolution of the Chandler and annual wobbles in a first-rate manner. They are important for geodynamical interpretations.

## Acknowledgement

Thanks to Dr Kevin Fleming for his linguistic advice that helped to improve the quality of this paper.

## References

Chandler, S.C.: On the variation of latitude. *Astron. J., 11 and 12*. Boston, 1891, 1892.

Chao, B.F.: Autoregressive harmonic analysis of the Earth's polar motion using homogeneous International Latitude Service data. *J. Geophys. Res., 88,* B12, p. 10299–10307, 1983.

Dick, S., McCarthy, D. and Luzum, B. (eds.): *Polar motion: Historical and scientific problems*. ASP Conf. Ser. Vol. 208. 641 pp. 2000.

Dickman, S.R.: Investigation of controversial polar motion features using homogeneous International Latitude Service data. *J. Geophys. Res. 86*, B6, p. 4904–4912, 1981.

Euler, L.: *Du Mouvement de Rotation des Corps Solides autour d'un Axe Variable*. Histoire de l'Académie Royale des Sciences et Belles Lettres, Berlin, 1758.

Gross, R.S.: *Combinations of Earth Orientation Measurements: SPACE 99, COMB99, and POLE99*. JPL Publication 00-5, Pasadena, California, 2000.

Guinot, B.: The Chandlerian wobble from 1900 to 1970. *Astron. Astrophys. 19*, p. 207–214, 1972.

Guinot, B.: The Chandlerian nutation from 1900 to 1980. *Geophys. J. R. Astron. Soc., 71*, p. 295–301, 1982.

Helmert, F.R., Albrecht, Th.: Der internationale Polhöhendienst. *Astron. Nachr., 148*, 3532, S. 49–56, 1899.

Höpfner, J.: Periodische Anteile in der Erdrotation und dem atmosphärischen Drehimpuls und ihre Genauigkeiten. *ZfV, 120*, S. 8–16, 1995a.

Höpfner, J.: Zur saisonalen Erregung der Polbewegung. *ZfV, 120*, S. 119–133, 1995b.

Höpfner, J.: Saisonale atmosphärische und nicht-atmosphärische Polbewegungsanteile. *ZfV, 120*, S. 502–508, 1995c.

Höpfner, J.: Polar motion at seasonal frequencies. *J. Geodynamics, 22*, p. 51–61, 1996.

Höpfner, J.: The International Latitude Service – a historical review, from the beginning to its foundation in 1899 and the period until 1922. *Surveys in Geophysics, 21*, p. 521–566, 2000.

Höpfner, J.: Parameter variability of the observed polar motions with smaller amplitudes. Paper presented at the XXVII General Assembly, EGS, Nice, France, 22–26 April 2002. *J. Geodesy* (in press), 2002.

Höpfner, J.: Chandler and annual wobbles based on space-geodetic measurements. Paper presented at the XXVI General Assembly, EGS, Nice, France, 26–30 March 2001. *J. Geodynamics* (in press), 2002a.

Höpfner, J.: Polar motions with a half-Chandler period and less in their temporal variability. Paper presented at the XXVI General Assembly, EGS, Nice, France, 26–30 March 2001. *J. Geodynamics* (in press), 2002b.

IERS: *1999 IERS Annual report*. Obs. de Paris, 2000.

Iijima, S.: On the yearly trend of the periodic components of polar motion. *Annals of the Tokyo Astron. Obs., 9*, p. 155–181, 1965.

Jahresbericht Preussen: Verh. der vom 15. bis 24. Oct. 1883 in Rom abgehaltenen Siebenten Allg. Conf. der Europäischen Gradmessung. Zugleich mit dem Generalbericht für das Jahr 1883. Berlin, 1884.

Kimura, H.: Variations in the fourteen months' component of the polar motion. *Monthly Notices R. Astron. Soc., 78*, p. 163, 1917.

Küstner, F.: *Neue Methode zur Bestimmung der Aberrations-Constante nebst Untersuchungen über die Veränderlichkeit der Polhöhe*. Beobachtungs-Ergebnisse der Königlichen Sternwarte zu Berlin, H. 3, 1888.

Lagrange, J.L.: *Mécanique Analitique*. Paris, 1788.

Lenhardt, H. and Groten, E.: Chandler wobble parameters from BIH and ILS data. *Manuscripta Geodaetica, 10*, p. 296–305, 1987.

Nastula, J., Korsun, A., Kołaczek, B., Kosek, W. and Hozakowski, W.: Variations of the Chandler and annual wobbles of polar motion in 1846–1988 and their prediction. *Manuscripta Geodaetica, 18*, p. 131–135, 1993.

Okubo, S.: Is the Chandler period variable? *Geophys. J. R. Astron. Soc., 71*, p. 629–646, 1982.

Peters, C.A.F.: Resultate aus Beobachtungen des Polarsterns am Ertelschen Verticalkreise der Pulkowaer Sternwarte. *Astron. Nachr., 22*, Nr. 509–512. Altona, 1844.

Poinsot, L.: Théorie Nouvelle de la Rotation des Corps. *L'Institut. Journal Général des Sociétés et Travaux Scientifiques, 2*. Paris, 1834.

Poinsot, L.: Théorie Nouvelle de la Rotation des Corps. *Journal de Mathématiques Pures et Appliquées, 16*. Paris, 1851.

Proverbio, E., Carta, F. and Mazzoleni, F.: *Analysis of the Chandler period of polar coordinates calculated with Orlov's method*. Pubblicazioni Della Stazione Astronomica Internazionale Di Latitudine Carloforte-Cagliari. Nuova Serie, N. 18, 1971.

Schuh, H., Nagel, S. and Seitz, T.: Linear drift and periodic variations observed in long term series of polar motion. *J. Geodesy, 74*, p. 701–710, 2001.

Vicente, R.O. and Wilson, C.R.: On the variability of the Chandler frequency. *J. Geophys. Res., 102*, B9, p. 20439–20445, 1997.

Vondrák, J.: Earth rotation parameters 1899.7-1992.0 after reanalysis within the Hipparcos frame. *Surveys in Geophysics, 20*, p. 169–195, 1999.

Vondrák, J., Pešek, I., Ron, C., and Čepek, A.: *Earth orientation parameters 1899.7-1992.0 in the ICRS based on the Hipparcos reference frame*. Publ. Astron. Inst. Acad. Sc. Czech Rep. 56 pp. 1998.

Wanach, B.: *Resultate des Internationalen Breitendienstes, Bd. V.*. Z.B. Internat. Erdmessung N.F. Veröff. Nr. 30. Berlin, 1916.

Wanach, B.: *Die Chandlersche und Newcombsche Periode der Polbewegung*. Z.B. Internat. Erdmessung. N.F. Veröff. Nr. 34. Berlin. 1919.

Wilson, C.R. and Vicente, R.O.: An analysis of the homogeneous ILS polar motion series. *Geophys. J. R. Astron. Soc., 62*, p. 605–616, 1980.

**Anschrift des Autors**

Dr.-Ing. habil. Joachim Höpfner
GeoForschungsZentrum Potsdam (GFZ)
Division Kinematics and Dynamics of the Earth
Telegrafenberg, D-14473 Potsdam
Germany
ho@gfz-potsdam.de
www.gfz-potsdam.de